JOURNAL OF VIROLOGY, Apr. 2010, p. 3464–3475 Vol. 84, No. 7
0022-538X/10/$12.00 doi:10.1128/JVI.02374-09

Glycosylation of PrP^C Determines Timing of Neuroinvasion and Targeting in the Brain following Transmissible Spongiform Encephalopathy Infection by a Peripheral Route▽

Enrico Cancellotti,[1]* Barry M. Bradford,[1] Nadia L. Tuzi,[1]† Raymond D. Hickey,[1]‡ Debbie Brown,[1] Karen L. Brown,[1] Rona M. Barron,[1] Dorothy Kisielewski,[1] Pedro Piccardo,[2] and Jean C. Manson[1]

Neuropathogenesis Division, The Roslin Institute and Royal (Dick) School of Veterinary Studies, University of Edinburgh, United Kingdom,[1] and Center for Biologics Evaluation and Research, Food and Drug Administration, Rockville, Maryland[2]

Received 11 November 2009/Accepted 12 January 2010

Transmissible spongiform encephalopathy (TSE) infectivity naturally spreads from site of entry in the periphery to the central nervous system where pathological lesions are formed. Several routes and cells within the host have been identified as important for facilitating the infectious process. Expression of the glycoprotein cellular PrP (PrP^C) is considered a key factor for replication of infectivity in the central nervous system (CNS) and its transport to the brain, and it has been suggested that the infectious agent propagates from cell to cell via a domino-like effect. However, precisely how this is achieved and what involvement the different glycoforms of PrP have in these processes remain to be determined. To address this issue, we have used our unique models of gene-targeted transgenic mice expressing different glycosylated forms of PrP. Two TSE strains were inoculated intraperitoneally into these mice to assess the contribution of diglycosylated, monoglycosylated, and unglycosylated PrP in spreading of infectivity to the brain. This study demonstrates that glycosylation of host PrP has a profound effect in determining the outcome of disease. Lack of diglycosylated PrP slowed or prevented disease onset after peripheral challenge, suggesting an important role for fully glycosylated PrP in either the replication of the infectious agent in the periphery or its transport to the CNS. Moreover, mice expressing unglycosylated PrP did not develop clinical disease, and mice expressing monoglycosylated PrP showed strikingly different neuropathologic features compared to those expressing diglycosylated PrP. This demonstrates that targeting in the brain following peripheral inoculation is profoundly influenced by the glycosylation status of host PrP.

Transmissible spongiform encephalopathies (TSE) or prion diseases are a group of fatal neurodegenerative diseases which include Creutzfeldt-Jakob disease (CJD) in humans, scrapie in sheep and goats, bovine spongiform encephalopathies (BSE) in cattle, and chronic wasting disease (CWD) in deer and elk (30). These diseases can be sporadic, familial, or acquired by infection, and the common hallmark is a distinct pathology in the central nervous system (CNS) characterized by neuronal loss, spongiform degeneration, and gliosis (38, 46).

Expression of the host-encoded cellular PrP (PrP^C) is fundamental for the onset of disease since PrP-deficient mice are refractory to TSE infection (11, 31). PrP^C is a glycoprotein with two consensus sites for attachment of N-linked glycans (at codons 180 and 196 in the mouse) which are variably occupied, producing di-, mono-, and unglycosylated PrP (43). The diversity in glycosylation, combined with the complexity of added sugars, results in a large number of glycosylated forms of PrP (41). A central event associated with TSE infection is the conformational conversion of PrP^C into an abnormal protease-resistant form, PrP^{Sc} (39). PrP^{Sc} is deposited in brain and, in some but not all cases, in peripheral organs of individuals affected by TSE (21).

Although the pathology associated with TSE is found in the brain, the periphery is the most natural route of acquiring infection. Evidence suggests that oral transmission via contaminated food is linked with transmission of BSE to humans, resulting in variant CJD (vCJD) (10, 47), and blood transfusion has been identified as a probable route of human-to-human transmission of vCJD (23, 27, 36). Moreover, parenteral administration of contaminated human tissue-derived therapeutics has been shown to facilitate iatrogenic spread of these diseases (8, 46). It is therefore important to understand the mechanisms that allow the infectious agent to propagate in the periphery and be transported to the CNS prior to the onset of neurodegeneration in the brain.

Many studies have been conducted to understand routes of transmission (for a review see references 1 and 29). Lymphoid tissues such as the spleen have been shown to play a fundamental role in agent replication and propagation in the very early stages of disease. Indeed, studies of splenectomized and asplenic mice have shown the lymphoreticular system (LRS) to be an important site for TSE agent replication (14, 26). The periphery also appears to have a role in processing the infectious agent following intracerebral (i.c.) inoculation as PrP^{Sc} accumulates in the spleen shortly after inoculation and before accumulation of the abnormal protein in the brain (15, 17). Within the LRS, follicular dendritic cells (FDC) have been

* Corresponding author. Mailing address: The Roslin Institute and R(D)SVS University of Edinburgh, Roslin, Midlothian EH25 9PS, Scotland, United Kingdom. Phone: 44 131 527 4200. Fax: 44 131 440 0434. E-mail: enrico.cancellotti@roslin.ed.ac.uk.

† Present address: Biology Teaching Organisation, University of Edinburgh, United Kingdom.

‡ Present address: Department of Molecular and Medical Genetics, Oregon Health and Science University, Portland, OR.

▽ Published ahead of print on 27 January 2010.

shown to be important for the uptake of infectivity and subsequent spreading toward the CNS (7, 28, 33, 35). Several studies have also suggested the peripheral nervous systems (PNS) as a potential route of infectivity to the brain, implicating the vagus and sciatic nerves in this process (5, 20, 25, 34).

Expression of PrP^C in the peripheral tissues appears to be an important prerequisite for the transport of infectivity to the CNS following peripheral routes of inoculation. Indeed, it has been proposed that a continuous chain of cells expressing PrP^C is fundamental for TSE neuroinvasion (6, 40), with overexpression of endogenous PrP in the PNS greatly facilitating the spread of infectivity (19). Thus, host PrP appears to have a fundamental role in the uptake, transport, and replication of the infectious agent (6). Moreover, it has been suggested that the different PrP^C glycoforms may influence the timing of neuroinvasion by directly influencing the interaction with the infectious agent (19). However, the mechanism by which the different glycoforms are involved in these processes remains to be determined.

In order to investigate the role of PrP^C glycosylation in TSE disease after peripheral infection with different TSE strains, we have used our inbred gene-targeted transgenic mice expressing different glycosylated forms of PrP. These mice expressed PrP with no sugars at the first (designated G1/G1 in homozygous mice) or the second glycosylation site (G2/G2) or both (G3/G3) under the control of the endogenous PrP promoter (13). We have previously shown that following intracerebral inoculation, all glycotypes are susceptible to infection with at least one TSE strain and that the type of PrP glycosylation in the host influenced the incubation period but not the distribution of pathological lesions in the brain (45). Here, we examine the influence of host PrP glycosylation on the peripheral acquisition of infection and demonstrate that, unlike the intracerebral route, mice without PrP glycosylation were resistant to disease and that the different glycoforms had a profound influence on not only the timing of disease but also the type and distribution of the PrP^{Sc} deposits in the brain.

MATERIALS AND METHODS

Transgenic mouse lines. Inbred gene-targeted transgenic mouse lines G1, G2, and G3, and the corresponding inbred 129/Ola wild-type control line have been described previously (13). Edinburgh PrP null mice (31) were used as negative controls.

Genotyping of mouse tail DNA. All the transgenic mice used in this study were genotyped twice: before inoculation and at the end of the experiments. A portion of tail was removed from each mouse. DNA was prepared from a 1-cm piece of tail by digestion overnight at 37°C in tail lysis buffer (300 mM sodium acetate, 1% SDS, 10 mM Tris, pH 8, 1 mM EDTA, 200 μg/ml proteinase K) and subsequent extraction with an equal volume of phenol-chloroform. DNA was precipitated with isopropanol, washed with 70% ethanol, and resuspended in 100 μl of TE buffer (10 mM Tris, 1 mM EDTA, pH 7.4). The mismatch PCR method to identify the different transgenics has been described elsewhere (13).

Preparation of inoculum and injection. Inocula were prepared from the brains of C57BL mice with terminal ME7 or 79A (mouse-adapted scrapie strains) TSE disease. A 1% homogenate of each sample was prepared in sterile saline prior to use as an inoculum. All experimental protocols were submitted to the Local Ethical Review Committee for approval before mice were inoculated. All experiments were performed under license and in accordance with the United Kingdom Home Office Regulations under the Animals (Scientific Procedures) Act, 1986.

Scoring of clinical TSE disease. The presence of clinical TSE disease was assessed as described previously (16). Animals were scored for clinical disease without reference to the genotype of the mouse. Genotypes were confirmed for each animal by PCR analysis of tail DNA at the end of the experiment. Incubation times were calculated as the interval between inoculation and culling due to terminal TSE disease. Mice were killed by cervical dislocation at the terminal stage of disease, at termination of the experiment (between 500 and 700 days), or for welfare reasons due to intercurrent illness.

Lesion profiles. Sections were stained with hematoxylin and eosin and scored for vacuolar degeneration on a scale of 0 to 5 in nine standard gray matter areas and on a scale of 0 to 3 in three standard white matter areas as described previously (16).

Immunohistochemical analysis in brain. Sections were stained for disease associated PrP using monoclonal antibody 6H4 (1/1,000; Prionics). Antigen retrieval by autoclaving at 121°C for 15 min and 10 min in formic acid (98%) was used to facilitate detection of the antigens. Sections were then blocked with normal serum prior to incubation with the primary antibody. Antibody binding was detected with a catalyzed signal amplification system (Dakocytomation) and visualized with diaminobenzidine (DAB). In all the experiments normal brain homogenate inoculum and PrP null negative controls were used. Images were taken using a Nikon Eclipse E800 microscope. Sections were analyzed by an observer blinded to the mouse genotype and type of inoculum.

PrP^{Sc} extraction from spleens. Mice were killed by cervical dislocation; spleens were removed, flash frozen in liquid nitrogen, and stored at −70°C until required. Whole spleens were weighed, and PrP^{Sc} was extracted using the method of centrifugal concentration from detergent solution (15). The spleen was homogenized in 3 ml of 0.2 M potassium chloride and 20 μl of 100 mM phenylmethylsulfonyl fluoride (PMSF) and centrifuged at 1,500 rpm for 10 min, and the subsequent supernatant was centrifuged at 50,000 rpm for 30 min, all at 4°C. This pellet was resuspended in 2 ml of 0.1 M Tris-hydrochloric acid (Tris-HCl, pH 7.4), and the suspension was divided into two equal parts: one part was left at 4°C with 40 μl of 100 mM PMSF for samples that were not digested with proteinase K (−PK; Sigma), and the other part was incubated with 3 μl of 18 mg/ml PK at 37°C for the samples digested with PK (+PK), both for 1 h. Twenty microliters of PMSF, 1 ml of 2% sarcosyl, and 2 μl of β-mercaptoethanol were added, and the samples were incubated at 37°C for an additional 1 h. The samples were then overlaid on 200 μl of 20% sucrose and centrifuged at 50,000 rpm for 2 h, and the pellets were stored at −20°C.

Western blotting. Mice were killed by cervical dislocation, and brains and spleens were removed, flash frozen in liquid nitrogen, and then stored at −70°C until required. Spleen preparation has already been described above. Brain homogenates (10%, wt/vol) were prepared in NP-40 lysis buffer (1% Nonidet P-40, 0.5% sodium deoxycholate, 150 mM NaCl, 50 mM Tris-HCl, pH 7.5, and 1 mM PMSF). The homogenate was centrifuged at 16,000 rpm for 10 min at 4°C, and supernatant was isolated. Total protein was denatured in 1× Novex Tris-glycine SDS sample buffer (Invitrogen Life Technologies) and 1× NuPage sample reducing agent (Invitrogen Life Technologies) for 30 min at 95°C. Proteins were separated by gel electrophoresis at 125 V using 12% Novex Tris-glycine gels (Invitrogen Life Technologies). Proteins in the acrylamide gel were transferred to polyvinylidene difluoride (PVDF) membrane at 2 mA/cm^2 of gel using a semidry transfer blotter (Bio-Rad) in 1× transfer solution (48 mM Tris, 39 mM glycine, 0.375% SDS, 20% methanol). Presence of PrP was assessed using the anti-PrP monoclonal antibodies 8H4 or 7A12 (1/10,000; kind gift of M. S. Sy) (48).

Immunohistochemical analysis of spleens. Tissues were flash frozen in liquid nitrogen and embedded in optimal cryotomy temperature (OCT) compound prior to sectioning on a Leica cryostat. Serial sections (10 μm) were cut and air dried overnight on SuperFrost Plus slides. Sections were fixed in acetone for 10 min. All labeling was done at room temperature in a humid chamber. For light microscopy, sections were blocked in normal mouse serum (1/20) for 15 min prior to incubation for 60 min with the primary antibody: 8H4 for PrP detection or the rat anti-mouse FDC-M2 monoclonal antibody for FDC (1/800; AMS Biotechnology). After being washed in Tris (pH 7.6)-bovine serum albumin (BSA) buffer, sections were further incubated for 60 min in mouse anti-rat biotinylated serum (1/500; Jacksons). After further washing, sections were stained with streptavidin-alkaline phosphatase reagent and then Vector red alkaline phosphatase substrate (Vector) according to the manufacturer's protocols. Finally, sections were counterstained with hematoxylin and rinsed in Scott's tap water prior to dehydration and mounting. Confocal microscopic studies were performed in sections probed with antibodies CD16/CD32 at a 1/100 dilution (BD Biosciences). Following washing in Tris (pH 7.6)-BSA buffer, sections were further incubated for 60 min in mouse anti-rat biotinylated serum (1/500; Jacksons). After further washing, sections were incubated with streptavidin-Alexa Fluor 594 (1/200; Abcam) for 60 min prior to mounting in fluorescent mounting medium (Dako). For double immunolabeling of FDC and PrP^C, sections were initially blocked in normal goat serum (1/20) for 20 min prior to an overnight incubation with the anti-PrP antibody 1B3 (1/1,000; kind gift of C. Farquhar),

TABLE 1. Incubation periods of Wt and glycosylation mutant homozygous mice infected intraperitoneally with strain 79A or ME7

Genotype	Strain	Result of i.p. inoculation			Result of i.c. inoculation[a]	
		Incubation time (avg no. of days ± SEM)	No. of clinically and pathologically positive animals/ total no. of mice	Difference in incubation time relative to the Wt (days)	Incubation time (avg no. of days ± SEM)	Difference in incubation time relative to the Wt (days)
Wt	79A	201 ± 2.2	19/20		148 ± 2.6	
G1/G1	79A	310 ± 35	11/18	+109	194 ± 21	+46
G2/G2	79A	307 ± 4.5	14/14	+106	167 ± 9.3	+19
G3/G3	79A	>700	0/14	>500	435 ± 92	+287
Wt	ME7	257 ± 3	18/19		163 ± 2	
G1/G1	ME7	>700	0/11	>500	>600	>400
G2/G2	ME7	280 ± 4	23/25	+23	160 ± 2.5	−3
G3/G3	ME7	>700	0/16	>500	>700	>500

[a] Results for i.c. inoculation (from reference 45) are shown for comparison.

followed by incubation with the fluorescent secondary antibody goat anti-rabbit Alexa Fluor 488 (1/200; Abcam) for 60 min. After repeated washings, sections were subsequently blocked with normal mouse serum (1/20) for 20 min prior to a 60-min incubation in the second primary antibody, FDC-M2 (1/1,000), followed by a 60-min incubation in mouse anti-rat biotinylated serum (1/500). Incubation with the fluorescent antibody streptavidin-Alexa Fluor 594 (1/200; Abcam) for 60 min preceded mounting in fluorescent mounting medium. Control sections, with normal rabbit or rat serum substituted for the primary antibody, were included in all immunostaining experiments.

Thioflavin-S treatment. Brain sections were stained with hematoxylin for 30 s and then washed in water. Sections were treated with a thioflavin-S solution (10 mg/ml) for 5 min and then immersed in 70% ethanol solution for 5 min. After sections were rinsed in water, they were mounted using fluorescent mounting medium (Dakocytomation) and analyzed using a Hamamatsu camera and Image Pro Plus.

RESULTS

Host PrP glycosylation regulates the timing of TSE neuroinvasion. To assess the effect of glycosylation in the TSE trafficking following peripheral exposure, wild-type and glycosylation-deficient mice were inoculated intraperitoneally (i.p.) with the ME7 or 79A mouse-adapted scrapie strain and monitored for the appearance of clinical signs of disease (16). G2 homozygous mice (G2/G2) showed a very long incubation period of disease compared to wild-type mice following i.p. inoculation with 79A. All G2/G2 animals succumbed to TSE disease, with an average incubation period of 307 (± 4.5) days, whereas the average incubation period in wild-type animals was 201 (± 2.2) days (Table 1). However, inoculation of G2/G2 mice with ME7 produced only a modest increase in the incubation period, with an average of 280 (±4) days compared to 257 ± 3 days for wild-type mice inoculated with the same strain (Table 1). Thus, lack of sugars at the second site delays the onset of disease, but the extent of this delay is TSE strain specific.

A very long incubation period and low susceptibility were also observed in G1 homozygous mice (G1/G1) inoculated i.p. with 79A compared with the wild-type mice. In this case only 11/18 G1 animals succumbed to disease, with an average incubation period of 310 (± 35) days (Table 1), whereas no G1/G1 mice showed any clinical disease signs after more than 700 days following peripheral administration of ME7. No clinical signs of disease were observed in G3 homozygous mice (G3/G3) after i.p. inoculation with either ME7 or 79A (Table 1). Therefore, host PrP glycosylation clearly influences the incubation time and susceptibility to disease following an intraperitoneal inoculation.

Glycosylation state of PrP^C in the host determines the targeting of pathological lesions in the brain following peripheral infection. Western blot analysis using the anti-PrP antibodies 8H4 or 7A12 revealed the presence of PK-resistant unglyco-

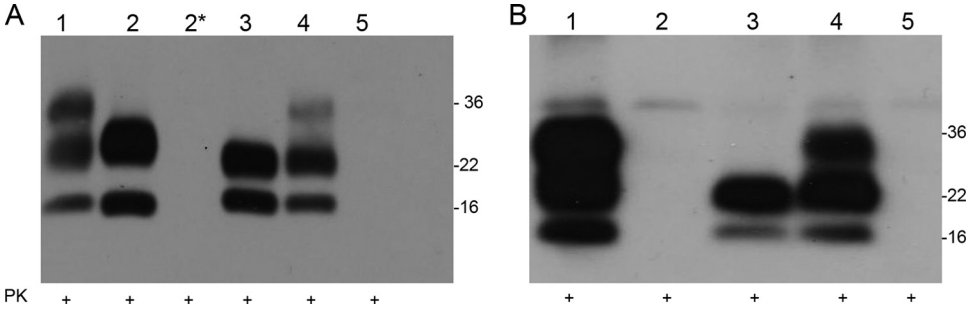

FIG. 1. Presence of PrP^{Sc} in brain of peripherally inoculated mice. In order to detect presence of proteinase K-resistant PrP, Western blotting using the 7A12 anti-PrP antibody was carried out in brains from clinically positive and clinically negative mice after injections with 79A or ME7. Brain homogenates from the different genotypes were treated with PK prior to SDS-PAGE analysis and immunoblotting. (A) Brains after peripheral infection with strain 79A. This analysis revealed presence of PK-resistant PrP in the brain of clinically positive Wt/Wt, G1/G1, G2/G2, and Wt/G2 mice but not in brains of clinically negative G1/G1 and G3/G3 mice. (B) Mouse brains after peripheral infection with strain ME7. This analysis revealed the presence of PK-resistant PrP in brains of clinically positive wild-type, G2/G2, and Wt/G2. However, no PK-resistant PrP was found in the brains of clinically negative G1/G1 and G3/G3 mice. Lane 1, wild type; lane 2, G1/G1; lane 2*, G1/G1 clinically negative; lane 3, G2/G2; lane 4, Wt/G2; lane 5, G3/G3.

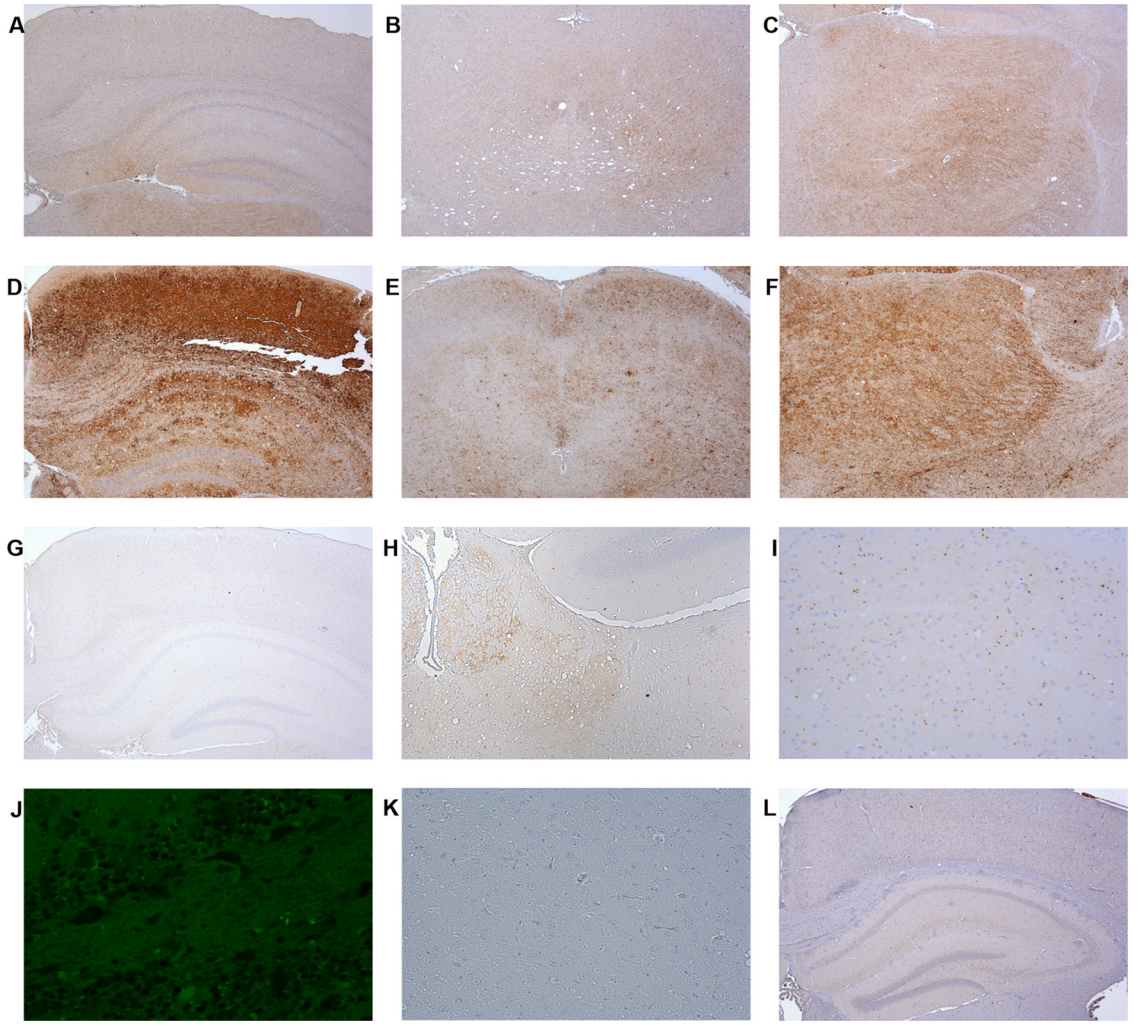

FIG. 2. PrP^{Sc} deposition in brain of wild-type and transgenic homozygous mice after peripheral administration of 79A. Brains from clinically positive and clinically negative mice after 79A challenge were immunostained for PrP^{Sc} with the monoclonal antibody 6H4 and analyzed by light microscopy using a Nikon Eclipse E800 microscope. (A to C) Wild-type animal brain showing a characteristic fine punctate PrP deposition. In these mice little involvement of the hippocampus and cortex areas (A) and of the midbrain (B) was observed, with most of the PrP^{Sc} deposition present in the thalamus (C). (D to F) G2/G2 brains showing a very strong mantle-like PrP^{Sc} deposition in several brain regions such as cortex and hippocampus (D), midbrain (E), and thalamus (F). (G to K) G1/G1 mouse brain showing a very peculiar PrP^{Sc} deposition characterized by aggregates of PrP^{Sc} in very specific brain regions. In contrast to G2/G2 mice, G1 animals did not show any PrP^{Sc} deposition in many brain areas, including the hippocampus and cortex (G). However, some PrP^{Sc} deposition in the form of fine punctuate deposits was observed in the habenula (H). A closer examination of these brains revealed the presence also of unusual PrP^{Sc} small aggregates in the thalamus (I) that were thioflavin-S negative (J). These aggregates were PrP^{Sc} specific since they were not present in control brain sections treated just with normal mouse serum without any anti-PrP antibody (K). (L) G3/G3 clinically negative brain showing no PrP deposition in any area of the brain examined. Magnifications, ×4 (A to G, J, and L), ×10 (H), and ×20 (I).

sylated and monoglycosylated PrP^{Sc} in brains of all clinically positive G2/G2 animals inoculated with either ME7 or 79A (Fig. 1). A PK-resistant PrP^{Sc} characterized by lack of the diglycosylated band was also detected in 11 out of 18 clinically positive G1/G1 mice inoculated with 79A but not in the seven clinically negative G1/G1 animals after inoculation with the same strain (Fig. 1A). No PrP^{Sc} was detected in brain from G1/G1 mice inoculated with ME7 (Fig. 1B), and this was also the case for G3/G3 mouse brains after challenge with 79A or ME7 (Fig. 1).

PrP^{Sc} deposition was assessed in the brains of mice inoculated with 79A and ME7 strains by immunohistochemistry (IHC) using 6H4 antibody. This analysis revealed a remarkable difference in both the amount and distribution of PrP^{Sc} deposition between wild-type mice and G2/G2 mice injected with 79A. In wild-type mice a mild to moderate, fine punctate PrP^{Sc} immuno-positivity was observed in the thalamus and midbrain. Sparse PrP^{Sc} deposits were also occasionally seen in other brain areas (Fig. 2A to C). In G2/G2 animals fine punctate PrP^{Sc} immuno-positive deposits were seen in several brain regions: septum, thalamus, hippocampus, hypothalamus, midbrain, and brain stem. In several G2/G2 mice high levels of PrP^{Sc} accumulation were also observed in the cerebral cortex, whereas in wild-type animals this area of the brain had only sparse or no PrP^{Sc} deposition (Fig. 2D to F).

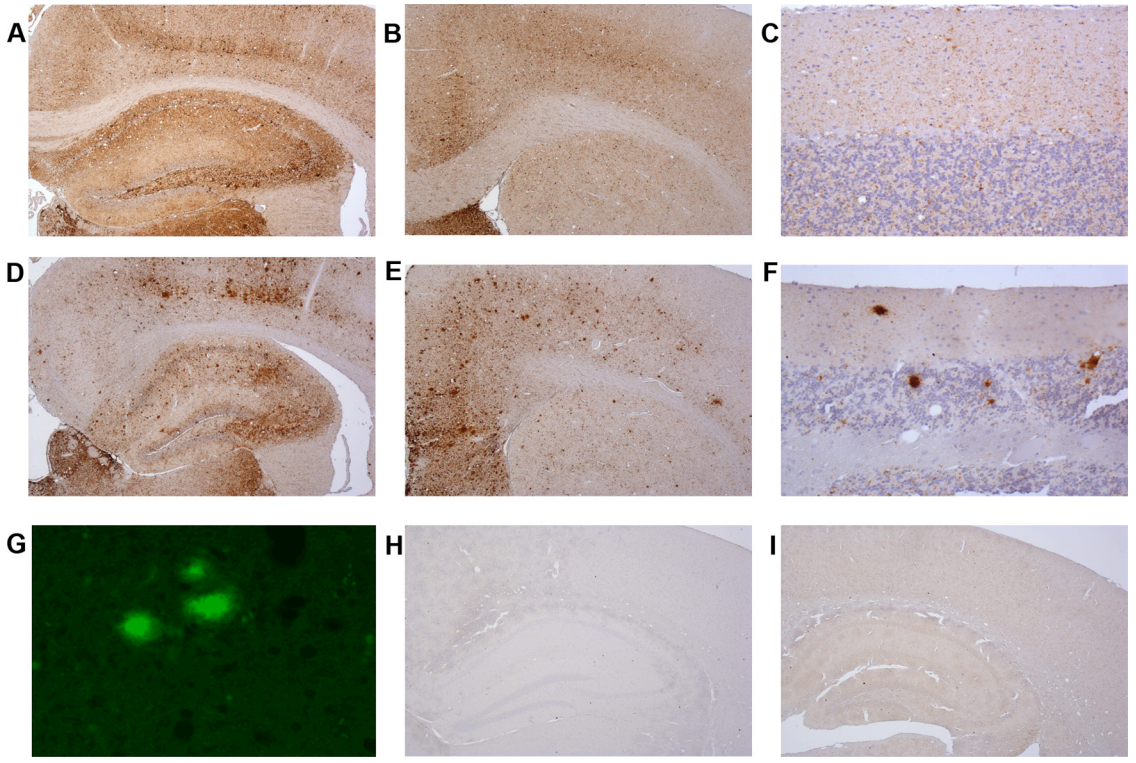

FIG. 3. PrP^{Sc} deposition in brain of wild-type and transgenic homozygous mice after peripheral administration of ME7. Brains from clinically positive and clinically negative mice after ME7 challenge were immunostained for PrP with the monoclonal antibody 6H4 and analyzed by light microscopy using a Nikon Eclipse E800 microscope. (A to C) Wild-type animal brains characterized by widespread fine punctate PrP^{Sc} deposition in several brain areas, such as cortex and hippocampus (A), septum (B), and cerebellum (C). (D to F) G2/G2 mice showing a different pattern of PrP^{Sc} deposition characterized by the presence of fine punctuate deposits and amyloid plaques in the cortex (D), septum (E), and cerebellum (F). Presence of amyloid plaques in these brains was confirmed by thioflavin-S treatment (G). (H and I) Brains of clinically negative G1/G1 (H) and G3/G3 (I) mice after ME7 challenge showing the absence of PrP^{Sc} deposition in every area of the brain examined. In panels H and I, the hippocampus and cortex areas are represented for both transgenic lines. Magnifications, ×4 (A, B, D, E, and G to I) and ×20 (C and F).

In ME7-inoculated wild-type animals, fine punctate and coarse (confluent) PrP^{Sc} immuno-positive deposits were seen in multiple brain areas including the septum, cerebral cortex, thalamus, hippocampus, hypothalamus, midbrain, brain stem, and cerebellum (Fig. 3A to C). Similar topographical distributions of fine punctate and coarse PrP^{Sc} deposits were observed in wild-type and G2/G2 mice. However, PrP^{Sc} deposition in the ME7-infected G2/G2 mice was also characterized by the presence of large, thioflavin S-positive amyloid plaques in all of the affected regions. (Fig. 3D to G).

The degree of spongiform degeneration in the CNS as determined by lesion profile analysis is an important parameter to define TSE disease (9). G2/G2 animals inoculated with 79A showed a higher degree of spongiform degeneration than wild-type mice in a number of areas of the gray matter: hypothalamus, thalamus, hippocampus, septum, and forebrain cortex. However, in other regions, such as cerebral cortex or medulla, no differences were observed. In the white matter areas analyzed (cerebellar white matter, mesencephalic tegmentum, and pyramidal tract), G2/G2 mice demonstrated a milder spongiosis (Fig. 4A). Differences in spongiform degeneration were also observed in G2/G2 mice inoculated with ME7, with more extensive spongiosis in the hypothalamus region in the transgenic mice than in wild-type mice and less in other areas such as the hippocampus, septum, cerebral cortex, and forebrain cortex in the gray matter and the pyramidal tract of the white matter (Fig. 4B).

An even more striking difference in pathology was observed in G1/G1 mice inoculated with 79A compared to wild-type animals in both the distribution and intensity of the PrP^{Sc} deposition and spongiosis. In the G1/G1 mice sparse, fine punctate PrP^{Sc} deposits were seen in habenula, thalamus, midbrain, and brain stem. In addition, coarse punctate PrP^{Sc} deposits were seen in the lateral thalamic region (Fig. 2G to I). To further investigate if this pattern was composed of amyloid deposits, infected G1/G1 mouse brain sections were treated with thioflavin-S (37). This analysis, however, did not reveal any fluorescent deposits in the parenchyma (Fig. 2J). A further unusual pathology in brain was also observed in these mice once a spongiform degeneration profile was performed. Indeed, in G1/G1 mouse brains spongiosis was restricted to the hypothalamus and dorsal medulla areas, whereas in wild-type mice a higher degree of spongiform degeneration was observed in all the gray and white matter regions analyzed (Fig. 4C). No spongiform degeneration or PrP^{Sc} deposition was found in any clinically negative G1/G1 and G3/G3 mice after inoculation with 79A or ME7, supporting the observation that these mice are resistant to peripheral inoculation with these strains (Fig. 2L and 3H and I).

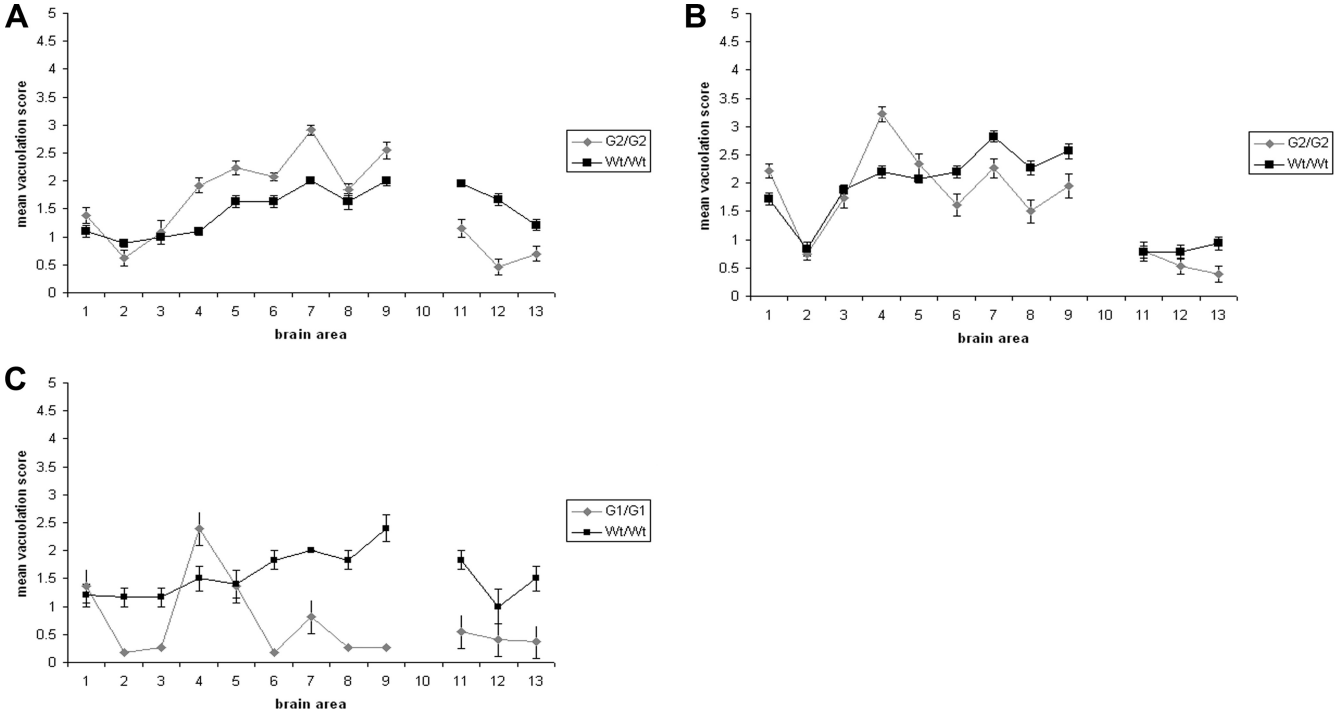

FIG. 4. Lesion profile analysis of wild-type and PrP glycosylation mutant homozygous mice after peripheral inoculation with 79A or ME7. Spongiform degeneration in brains of the clinically positive wild-type, G2, and G1 mice was analyzed after peripheral infection with 79A or ME7. For this purpose nine gray matter areas were scored on a scale of 0 to 5 (*y* axis). Gray matter areas are represented on the *x* axis by the following numbers: 1, dorsal medulla; 2, cerebellar cortex; 3, superior colliculus; 4, hypothalamus; 5, medial thalamus; 6, hippocampus; 7, septum; 8, cerebral cortex; and 9, forebrain cortex. Three white matter areas were scored on a scale of 0 to 3 (*y* axis). White matter areas are represented on the *x* axis by the following numbers: 11, cerebellar white matter; 12, mesencephalic tegmentum; and 13, pyramidal tract. The magnitude of spongiform degeneration in the transgenic mice was then compared with the one in wild-type mice. Graphs show lesion profile analysis of the brains of the mice indicated on the figure after infection with strains 79A (A and C) and ME7 (B). The mean score for each area is shown (error bars ± standard error of the mean [SEM]).

A single copy of wild-type PrP restores the incubation time in PrP glycosylation-deficient mice. Heterozygous mice expressing both wild-type and G2 PrP (Wt/G2) were also inoculated i.p. with 79A or ME7. Wt/G2 mice showed an incubation time strikingly similar to that of homozygous wild-type mice. Indeed, Wt/G2 mice inoculated with 79A died in an average incubation period of 205 (± 3) days, whereas wild-type animals succumbed with an average incubation period of 201 (± 2.2) days (Table 2). Similar incubation times were also observed between heterozygous and wild-type mice inoculated with ME7 (Wt/G2, 253 ± 5.5 days; Wt/Wt, 257 ± 2.8 days) (Table 2). Thus, a single copy of the wild-type *Prnp* gene was able to restore the incubation times of disease observed in the wild-type mice.

TABLE 2. Incubation periods of Wt and heterozygous Wt/G2 mice infected intraperitoneally with strain 79A or ME7

Genotype	Strain	Incubation time (avg no. of days ± SEM)	No. of clinically and pathologically positive animals/total no. of mice	Difference in incubation time relative to the Wt
Wt	79A	201 ± 2.2	19/20	
Wt/G2	79A	205 ± 3	23/26	+4
Wt	ME7	257 ± 3	18/18	
Wt/G2	ME7	253 ± 5	18/18	−4

Western blot analysis performed in brains of the clinically positive Wt/G2 heterozygous animals, after exposure to 79A or ME7, revealed the presence of PK-resistant diglycosylated PrP^{Sc}. The glycoprofile of PrP^{Sc} in these mice was characterized by having a monoglycosylated band more intense than the diglycosylated band (Fig. 1). This differs from the glycoprofile observed in wild-type homozygous animals characterized by a predominant diglycosylated band and reflects the glycosylation status of PrP^{C} in Wt/G2 mice.

Despite identical incubation times, immunohistochemical analysis of PrP^{Sc} deposition in brain sections revealed differences between wild-type and heterozygous animals. Analysis of brain sections from Wt/G2 mice inoculated with the 79A strain showed accumulation of PrP^{Sc} in several areas of the brain. However, the severe deposition of PrP^{Sc} in the cerebral cortex detected in G2/G2 mice was not apparent in heterozygous animals (Fig. 5A and B). Analysis of brain sections from Wt/G2 mice inoculated with the ME7 strain shows fine punctate PrP^{Sc} deposits in several areas. Moreover, coarse and plaque-like PrP^{Sc} deposits previously observed in G2/G2 mice were also present in the heterozygous animals; however, the size and numbers of these deposits were reduced compared to those seen in G2 homozygous animals (Fig. 5D and E). The

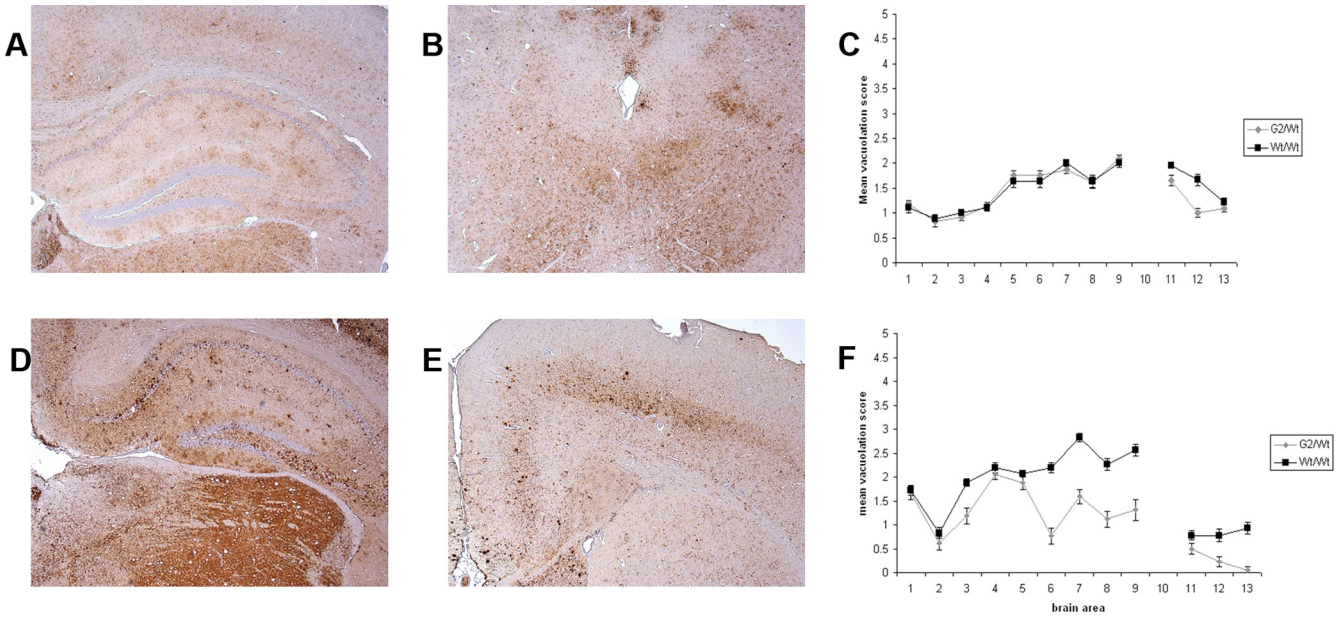

FIG. 5. Brain pathology analysis in G2 heterozygous animals challenged with 79A or ME7. Brains from clinically positive Wt/G2 heterozygous animals inoculated with 79A or ME7 were immunostained for PrP with monoclonal antibody 6H4 and analyzed by light microscopy using a Nikon Eclipse E800 microscope. Analysis of the spongiform degeneration in the nine gray matter areas and the three white matter areas described in the legend of Fig. 4 was also carried out in Wt/G2 brains and compared with spongiform degeneration in Wt/Wt mice. (A and B) Wt/G2 brain after inoculation with 79A i.p. showed a PrP deposition intermediate between that of wild-type and G2 homozygous animals. PrP^{Sc} accumulation was indeed observed in regions such as thalamus, hippocampus, and cerebral cortex (A) or midbrain (B). However, this deposition was less intense than the one observed in G2 homozygous animals (compare Fig. 2). (C) Although there were some differences in terms of PrP^{Sc} deposition between Wt/Wt and Wt/G2 mice, no differences were observed between these two lines in terms of spongiosis in all the brain areas analyzed. (D and E) Wt/G2 mice brains after peripheral infection with ME7 also resembled an intermediate pathology between wild-type and G2 homozygous animals. PrP^{Sc} deposits and small plaques were indeed observed in regions such as the hippocampus (D) and the septum (E) (compare Fig. 3). (F) Heterozygous animals presented a vacuolation profile that differed from that of wild-type mice infected with ME7, with lower degrees of vacuolation in several brain areas: 6, hippocampus; 7, septum; 8, cerebral cortex; and 9, forebrain cortex. Magnification, ×4 (A, B, D, and E).

immunohistochemical characteristics of PrP^{Sc} accumulation in heterozygous mice can be best described as intermediate between those seen in G2 and wild-type homozygous animals. The spongiform degeneration analysis revealed no differences in the brain areas affected between Wt/G2 and Wt/Wt mice inoculated with 79A (Fig. 5C). However, Wt/G2 mice inoculated with ME7 have reduced vacuolation in specific brain areas compared to wild-type mice, e.g., in the hippocampus, septum, cerebral cortex, forebrain cortex, and the pyramidal tract (Fig. 5F).

Glycosylation-deficient mice possess mature and functional FDC that express PrP^{C}. Since FDC have been suggested to be a pivotal component in the uptake and replication of infectivity in the periphery, we assessed if the delay or resistance observed in the glycosylation-deficient mice could be linked to any possible FDC abnormality.

FDC networks were detected using the FDC-M2 antibody. The epitope recognized by this antibody has been shown to be the activated form of the complement receptor C4 (44). FDC-M2 labels mature FDC networks within the germinal center as well as parts of the primary follicle. Initial light microscopy analysis revealed no overt differences between the FDC networks of transgenic and wild-type mice (Fig. 6A). To further explore the functionality of these networks, immunolabeling was carried out using an antibody which recognizes an epitope common to both CD16 and CD32, which are both low-affinity receptors for the immunoglobulin Fc portion expressed by functional FDC, as well as other cell types (18). No differences were evident in the labeling between the different genotypes (Fig. 6B).

It was then determined whether PrP^{C} localization within these FDC networks is altered in the transgenic mice compared with wild-type mice. For labeling of PrP^{C}, the rabbit polyclonal antibody used was 1B3, which targets the amino acid residues 14 to 36, 83 to 102, 119 to 139, and 188 to 212 on the PrP molecule (15). Confocal analysis of double immunofluorescent labeling of PrP and FDC networks showed that PrP^{C} colocalizes within the FDC networks of each of the transgenic genotypes and wild-type samples (Fig. 6C). Thus, the glycosylation-deficient mice, like wild-type mice, appear to possess an intact FDC network which expresses PrP^{C}.

Host PrP glycosylation influences the peripheral stages of TSE infectivity. Following peripheral inoculation of TSE-infected material, accumulation and amplification of infectivity in the LRS occur rapidly, with infectivity levels in these tissues reaching a plateau after several weeks (14–15). We therefore analyzed the presence of PrP^{Sc} deposition in spleens of clinically positive or clinically negative glycosylation-deficient transgenics and wild-type mice after i.p. inoculation with the 79A or ME7 strain by IHC. This analysis showed a correlation between the amount of PrP deposition in spleen and subsequent clinical disease. Clinically positive Wt/Wt and G2/G2 mice after 79A or ME7 infection or G1/G1 mice after 79A

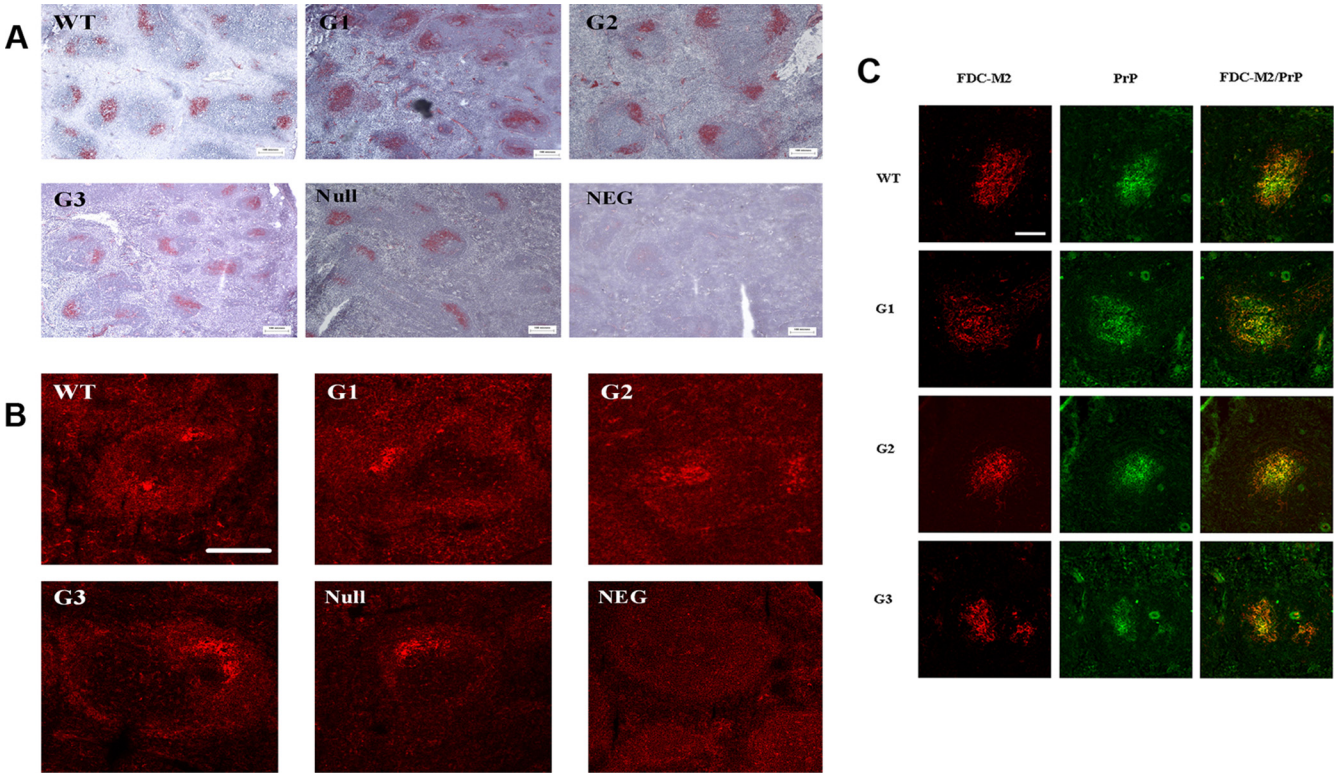

FIG. 6. Characterization of spleen morphology in glycosylation-deficient mice. In order to assess if a lack of sugars can induce an overt phenotype in spleen, a number of morphological assays in spleen derived from transgenic, wild-type, and PrP knockout animals (null) were performed. (A) FDC networks were detected using the FDC-M2 antibody, which labels mature FDC networks within the germinal center. With light microscopy analysis using a Nikon Eclipse E800 microscope, no differences were highlighted between wild-type and glycosylation-deficient mice. (B) CD16/CD32 antibody was used to investigate the functionality of FDC by confocal microscopy analysis. Again, there were no differences evident in the labeling between the different genotypes. Scale bar, 50 μm. (C) PrP localization within the FDC network was analyzed by confocal microscopy analysis. Double immunofluorescent labeling of PrP with 1B3 antibody (green) and of FDC networks with FDC-M2 antibody (red) showed that PrP^C colocalizes within the FDC networks (yellow) of each of the transgenic genotypes and wild-type samples. Scale bar, 50 μm.

challenge showed large amounts of PrP^{Sc} throughout the spleen (Fig. 7A to D and F). However, complete absence of PrP deposition was observed in spleens of clinically negative G1/G1 mice inoculated with ME7 and of clinically negative G3/G3 mice challenged with 79A or ME7 (Fig. 7E, G, and H). Very small PrP^{Sc} deposits in the spleen were also observed in some of the seven G1/G1 mice that were not affected by a clinical TSE disease after 79A challenge, suggesting that in these mice PrP^{Sc} amplification levels were not sufficient to further elicit TSE clinical disease (Fig. 7I).

Total lack of glycosylation in PrP^C prevents trafficking of PrP^{Sc} from brain to spleen. After intracerebral inoculation, PrP^{Sc} is often detected first in the spleen, suggesting that infectivity travels from the site of injection in the brain to the LRS and replicates in the periphery prior to causing disease in the CNS (15, 17). To test the influence of host PrP glycosylation in transport of PrP^{Sc} from brain to spleen, we analyzed by Western blotting the presence of PrP^{Sc} in spleens of the three glycosylation mutant mice infected intracerebrally in previous experiments (45) with ME7 and 79A. Wild-type and G2 mice are susceptible to infection with ME7, and PrP^{Sc} was detected in the spleens. However, G1/G1 and G3/G3 mice did not develop any clinical disease after challenge with ME7, and no PrP^{Sc} was detected in spleens (Fig. 8A), suggesting that lack of replication in the LRS may prevent clinical disease in these mice, as previously suggested (7). Presence of PrP^{Sc} was observed in the spleens of clinically positive G1/G1 and G2/G2 mice infected with 79A, but surprisingly no PrP^{Sc} was found in the spleens of G3/G3 mice that were clinically positive (Fig. 8B). These results suggest that monoglycosylated but not unglycosylated PrP is able to sustain transport of infectivity between the brain and the periphery and that while replication in the spleen is important for establishing disease with ME7 via intracerebral or intraperitoneal routes, this step may not be mandatory for establishing infection with 79A.

DISCUSSION

The mechanisms regulating peripheral propagation of the different TSE strains are not yet fully understood. Different organs, cells, and routes have been shown to be important according to which strain of agent is infecting a particular host. Some strains require amplification in the LRS before causing a productive infection in the CNS, whereas with other strains, such as naturally occurring BSE in cattle, the involvement of the LRS is limited (3–4, 12, 22, 42). A number of factors are likely to contribute to this diversity in neuroinvasion, including strain, host PrP genotype, and the route of entry. Our results

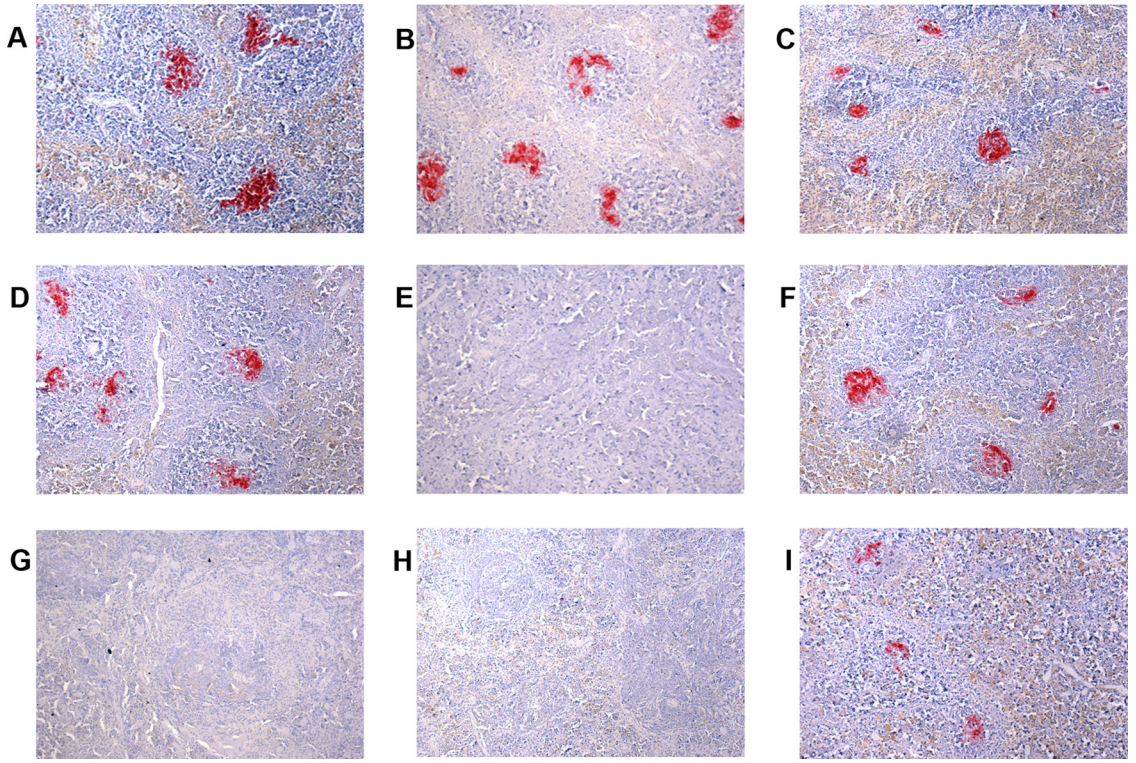

FIG. 7. PrP^{Sc} deposition in spleens of mice after peripheral inoculation with strain 79A or ME7. Spleens from clinically positive and clinically negative mice were immunostained for PrP with the monoclonal antibody 6H4 and analyzed by light microscopy using a Nikon Eclipse E800 microscope and a 10× objective. PrP^{Sc} deposition was observed in spleens of wild-type (A), G1/G1 (B), and G2/G2 (C) clinically positive animals after inoculation with 79A. PrP^{Sc} deposition was also observed in spleens of wild-type (D) and G2/G2 (F) clinically positive animals but not in G1/G1 clinically negative mice (E) after ME7 infection. PrP^{Sc} accumulation was also not observed in G3/G3 clinically negative mice after i.p. inoculation with either 79A or ME7 (G and H). Slight PrP^{Sc} deposition was observed in spleen of some clinically negative G1 mice after challenge with 79A (I).

now suggest that glycosylation status of the host PrP may be an important factor in this process and, in particular, in determining the timing of neuroinvasion and the final targeting in the CNS.

Glycosylated PrP^{C} appears to be required at the early stages of the infectious process, which may involve uptake and transport from the site of infection to the spleen or amplification of infectivity in the spleen. Clinical disease was observed in each of the PrP glycosylation-deficient mice following intracerebral inoculation with at least one strain (45), albeit with very long incubation periods and limited susceptibility in the G3 mice. In this study this was not the case as following intraperitoneal inoculation the G3 mice appeared to show complete resistance to infection with two different TSE strains.

This may be due to an inability of unglycosylated PrP^{C} to sustain the transport of infectivity from the periphery to the brain and/or vice versa. Therefore, PrP glycosylation plays a central role in the spread of infectivity from the periphery to the CNS. Moreover, our results suggest that replication or transport in the LRS is a limiting factor during spreading of TSE infectivity.

The role played by PrP^{C} glycotypes in the pathogenesis of disease appears to be strain specific. G2 mice developed disease after ME7 i.p. inoculation with only a short delay of 21 days compared to wild-type mice. Similarly, when ME7 was injected directly into the CNS, G2 mice developed TSE disease with incubation periods similar to those of wild-type mice (45). Thus, the monoglycosylated G2 PrP protein appears to be able to replicate and transport the ME7 agent almost as efficiently as the diglycosylated PrP. However, ME7 fails to establish disease following peripheral challenge of G1/G1 and G3/G3 mice, and PrP^{Sc} is absent from spleens and brains of these mice. This is in accordance with what was observed following direct inoculation of ME7 into the brain; although these transgenic mice did not develop any clinical TSE disease, G3 mice presented some degree of PrP deposition in the form of amyloid plaques (45). Thus, the first glycosylation site appears critical for the replication of ME7 in both the CNS and periphery. Failure to establish disease is therefore likely to be due to a failure of the host to replicate the agent.

G1 and G2 homozygous mice were susceptible to infection following peripheral challenge with 79A; however, the incubation time was more than 100 days longer than for wild-type animals. This delay after peripheral inoculation is much longer than that observed following inoculation of the same strain intracerebrally; in G1/G1 and G2/G2 mice the incubation of clinical prion disease was 40 and 20 days longer, respectively, than in wild-type mice (45). This suggests either that there is a difference in efficiency of replication of the agents in the pe-

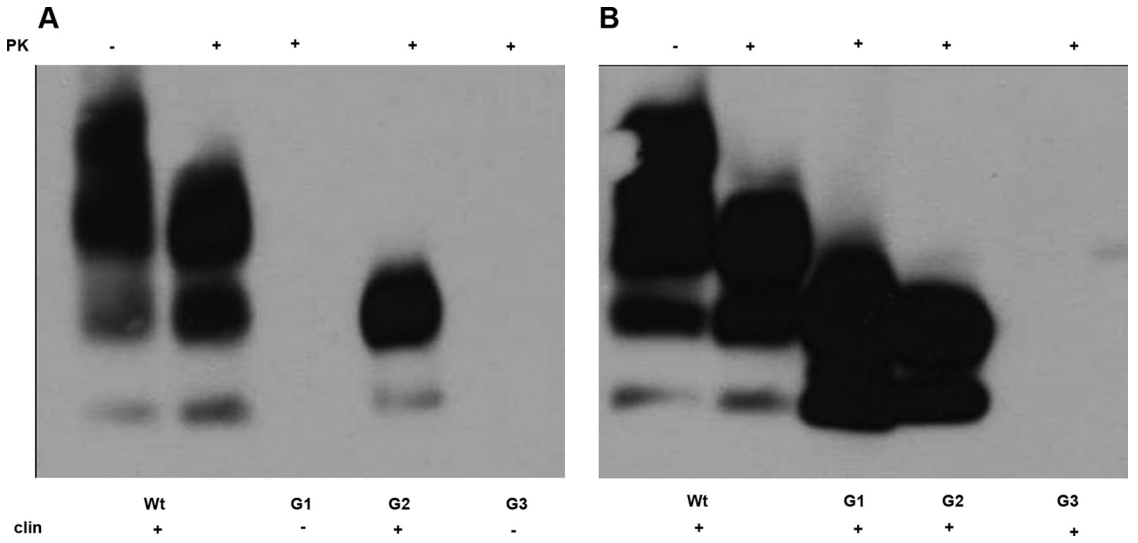

FIG. 8. Travel of PrP^{Sc} from brain to spleen. In order to assess influence of host PrP glycosylation in trafficking of PrP^{Sc} from the CNS to the periphery, spleens from glycosylation-deficient mice and wild-type animals inoculated intracranially with ME7 or 79A were tested for presence of PK-resistant PrP by Western blotting using the anti-PrP antibody 8H4. (A) Western blot analysis of spleen from mice infected i.c. with ME7 after pretreatment with PK. PK-resistant PrP was observed only in clinically positive wild-type and G2/G2 mice; no PrP^{Sc} was found in spleen of clinically negative G1/G1 and G3/G3 mice. (B) Western blot analysis of spleen from mice infected i.c. with 79A after pretreatment with PK. PrP^{Sc} was recovered in all clinically positive G1/G1, G2/G2, and wild-type mice; however, no PK-resistant PrP was found in clinically positive G3/G3 animals.

riphery and the CNS or that lack of diglycosylated protein in this case is delaying the transport to the CNS. However, the incubation time in G2 mice was rescued when a wild-type PrP was expressed alongside the monoglycosylated PrP. In heterozygous PrP mice a gene dosage effect on the length of TSE clinical disease onset was observed due to the contribution of both alleles. This effect was previously described in wild-type/knockout PrP heterozygous transgenic mice ($PrP^{+/-}$) in which the incubation time was almost doubled compared to incubation in PrP wild-type homozygous animals (32). In Wt/G2 mice it was therefore surprising to observe the appearance of clinical disease at the same time as in Wt/Wt mice when it might have been expected that incubation periods in these mice would fall somewhere between those of wild-type and G2 homozygous mice. This suggests that the mono- and diglycosylated forms of PrP can act together to facilitate replication and transport of the agent. This suggestion is also supported by the observation that heterozygous animals presented a brain pathology that was an intermediate between that observed in wild-type and G2 homozygous mice, indicating that both alleles are also contributing to the final targeting in brain. Thus, the provision of diglycosylated PrP clearly provides an important function in the disease process and can overcome the incubation time delays observed with only monoglycosylated and unglycosylated PrP. The discrepancy between the hybrid pathology and the wild-type incubation times observed in the heterozygote mice demonstrates that these are an important model for defining the mechanisms regulating the neuroinvasion of TSE infectivity, and further studies are under way to address this issue.

Host PrP glycosylation appears to determine the targeting in the CNS following peripheral challenge. Absence of fully glycosylated PrP had a profound effect in determining the brain area targeted by PrP^{Sc} deposition after infection with 79A. G1 mouse brains were characterized by PrP^{Sc} accumulation in very restricted areas like the habenula and the thalamus. This deposition was remarkably different from the characteristic widespread distribution of PrP^{Sc} in many brain areas observed in wild-type mice. G2 homozygous animals also presented changes in 79A targeting compared to wild-type animals, with cortex and midbrain heavily affected. This different targeting may be due to an effect of host PrP glycosylation in determining routes of propagation of infectivity from the periphery to the CNS or to the fact that the transgenic mice developed clinical disease with a much longer incubation time than the wild types. However, even in cases where there were modest alterations in the incubation times, in the glycosylation-deficient transgenic mice there were dramatic differences observed in PrP^{Sc} deposition. Absence of a fully glycosylated PrP appears to facilitate the deposition of amyloid plaque formation in the brain, compared with fine punctuate staining observed in wild-type mice after ME7 inoculation. This contrasts with the targeting in the brain following intracerebral challenge, where no difference in targeting was observed in the different lines of mice (45). After inoculation of 79A or ME7 directly into the brain, clinically positive G1/G1 and G2/G2 mice, indeed, did not present any differences in terms of spongiform degeneration or PrP^{Sc} deposition compared to wild-type animals. Wild-type and glycosylation-deficient mice had the same vacuolation profiles and the same widespread, fine punctuate PrP^{Sc} depositions throughout the brain (45). These results may also suggest that the delay observed in the transgenic animals may be due to an initial targeting of infectivity in different brain areas that may delay the neurotoxic effect, as previously proposed (24). Whether differences in routing to the CNS are responsible for the differences in targeting observed in the glycosylation-deficient mice remains to be established.

A difference in brain pathology between wild-type and gly-

cosylation-deficient mice was also confirmed by the analysis of vacuolation damage in the CNS. Differences were observed in G1 and G2 mice after infection with both 79A and ME7 in several brain areas. This analysis also revealed a discrepancy between PrP^{Sc} accumulation and spongiform degeneration. For example, the strong accumulation of PrP^{Sc} observed in the cortex of G2 but not of wild-type animals was not linked with a difference in terms of spongiosis in the same areas. This observation may support previous observations suggesting that PrP^{Sc} presence is not always associated with vacuolation (2, 37).

In summary, we have shown that PrP is a requirement for the peripheral events in TSE disease. In this process PrP glycosylation is a key component to determine the timing of neuroinvasion and the targeting in the CNS, and this effect varies according to TSE strain. Indeed, a fully glycosylated PrP molecule is required for the most efficient neuroinvasion by 79A. However, ME7, while less dependent on a fully glycosylated PrP, appears to be totally dependent on glycosylation at the first site. Finally, the results presented here indicating a role of N-linked glycans in the spread of TSE infectivity may have some important implications for the development of new therapeutic approaches. For example, destabilizing sugar-mediated interactions between host and the infectious agent would appear to provide an important approach to block propagation of infectivity.

ACKNOWLEDGMENTS

This work was supported by Biotechnology and Biological Science Research Council and Medical Research Council. R.D.H. was funded by Research in Life Sciences Program, University of Edinburgh.

We thank colleagues at The Roslin Institute and in particular all members of J. C. Manson's group for the useful discussions about this work; Robert Somerville and Abigail Diack for critical reading of the manuscript; Anne Coghill, Sandra Mack, and Gillian McGregor for assistance with the pathology analysis; Aileen Boyle for lesion profile analysis; and Irene McConnell, Val Thompson, Simon Cumming, Leanne Frame, and Kris Hogan for the breeding, care, injections, and the clinical scoring of the mice. 1B3 antibody was kindly provided by Christine Farquhar (The Roslin Institute, University of Edinburgh); 8H4 and 7A12 antibodies were kindly provided by Man-Sun Sy (Case Western Reserve University).

The findings and conclusions in this article have not been formally disseminated by the Food and Drug Administration and should not be construed to represent any Administration determination or policy.

REFERENCES

1. **Aguzzi, A., and M. Heikenwalder.** 2006. Pathogenesis of prion diseases: current status and future outlook. Nat. Rev. Microbiol. **4:**765–775.
2. **Barron, R. M., S. L. Campbell, D. King, A. Bellon, K. E. Chapman, R. A. Williamson, and J. C. Manson.** 2007. High titers of transmissible spongiform encephalopathy infectivity associated with extremely low levels of PrPSc in vivo. J. Biol. Chem. **282:**35878–35886.
3. **Beekes, M., and P. A. McBride.** 2000. Early accumulation of pathological PrP in the enteric nervous system and gut-associated lymphoid tissue of hamsters orally infected with scrapie. Neurosci. Lett. **278:**181–184.
4. **Beekes, M., and P. A. McBride.** 2007. The spread of prions through the body in naturally acquired transmissible spongiform encephalopathies. FEBS J. **274:**588–605.
5. **Beekes, M., P. A. McBride, and E. Baldauf.** 1998. Cerebral targeting indicates vagal spread of infection in hamsters fed with scrapie. J. Gen. Virol. **79:**601–607.
6. **Blattler, T., S. Brandner, A. J. Raeber, M. A. Klein, T. Voigtlander, C. Weissmann, and A. Aguzzi.** 1997. PrP-expressing tissue required for transfer of scrapie infectivity from spleen to brain. Nature **389:**69–73.
7. **Brown, K. L., K. Stewart, D. L. Ritchie, N. A. Mabbott, A. Williams, H. Fraser, W. I. Morrison, and M. E. Bruce.** 1999. Scrapie replication in lymphoid tissues depends on prion protein-expressing follicular dendritic cells. Nat. Med. **5:**1308–1312.
8. **Brown, P., M. Preece, J. P. Brandel, T. Sato, L. McShane, I. Zerr, A. Fletcher, R. G. Will, M. Pocchiari, N. R. Cashman, J. H. d'Aignaux, L. Cervenakova, J. Fradkin, L. B. Schonberger, and S. J. Collins.** 2000. Iatrogenic Creutzfeldt-Jakob disease at the millennium. Neurology **55:**1075–1081.
9. **Bruce, M. E.** 2003. TSE strain variation. Br. Med. Bull. **66:**99–108.
10. **Bruce, M. E., R. G. Will, J. W. Ironside, I. McConnell, D. Drummond, A. Suttie, L. McCardle, A. Chree, J. Hope, C. Birkett, S. Cousens, H. Fraser, and C. J. Bostock.** 1997. Transmissions to mice indicate that "new variant" CJD is caused by the BSE agent. Nature **389:**498–501.
11. **Bueler, H., A. Aguzzi, A. Sailer, R. A. Greiner, P. Autenried, M. Aguet, and C. Weissmann.** 1993. Mice devoid of PrP are resistant to scrapie. Cell **73:**1339–1347.
12. **Buschmann, A., and M. H. Groschup.** 2005. Highly bovine spongiform encephalopathy-sensitive transgenic mice confirm the essential restriction of infectivity to the nervous system in clinically diseased cattle. J. Infect. Dis. **192:**934–942.
13. **Cancellotti, E., F. Wiseman, N. L. Tuzi, H. Baybutt, P. Monaghan, L. Aitchison, J. Simpson, and J. C. Manson.** 2005. Altered glycosylated PrP proteins can have different neuronal trafficking in brain but do not acquire scrapie-like properties. J. Biol. Chem. **280:**42909–42918.
14. **Dickinson, A. G., and H. Fraser.** 1972. Scrapie: effect of Dh gene on incubation period of extraneurally injected agent. Heredity **29:**91–93.
15. **Farquhar, C. F., J. Dornan, R. A. Somerville, A. M. Tunstall, and J. Hope.** 1994. Effect of Sinc genotype, agent isolate and route of infection on the accumulation of protease-resistant PrP in non-central nervous system tissues during the development of murine scrapie. J. Gen. Virol. **75:**495–504.
16. **Fraser, H., and A. G. Dickinson.** 1967. Distribution of experimentally induced scrapie lesions in the brain. Nature **216:**1310–1311.
17. **Fraser, J. R.** 1996. Infectivity in extraneural tissues following intraocular scrapie infection. J. Gen. Virol. **77:**2663–2668.
18. **Gessner, J. E., H. Heiken, A. Tamm, and R. E. Schmidt.** 1998. The IgG Fc receptor family. Ann. Hematol. **76:**231–248.
19. **Glatzel, M., and A. Aguzzi.** 2000. PrP(C) expression in the peripheral nervous system is a determinant of prion neuroinvasion. J. Gen. Virol. **81:**2813–2821.
20. **Glatzel, M., F. L. Heppner, K. M. Albers, and A. Aguzzi.** 2001. Sympathetic innervation of lymphoreticular organs is rate limiting for prion neuroinvasion. Neuron **31:**25–34.
21. **Glatzel, M., K. Stoeck, H. Seeger, T. Luhrs, and A. Aguzzi.** 2005. Human prion diseases: molecular and clinical aspects. Arch. Neurol. **62:**545–552.
22. **Heggebo, R., C. M. Press, G. Gunnes, L. Gonzalez, and M. Jeffrey.** 2002. Distribution and accumulation of PrP in gut-associated and peripheral lymphoid tissue of scrapie-affected Suffolk sheep. J. Gen. Virol. **83:**479–489.
23. **Houston, F., S. McCutcheon, W. Goldmann, A. Chong, J. Foster, S. Siso, L. Gonzalez, M. Jeffrey, and N. Hunter.** 2008. Prion diseases are efficiently transmitted by blood transfusion in sheep. Blood **112:**4739–4745.
24. **Kimberlin, R. H., S. Cole, and C. A. Walker.** 1987. Pathogenesis of scrapie is faster when infection is intraspinal instead of intracerebral. Microb. Pathog. **2:**405–415.
25. **Kimberlin, R. H., and C. A. Walker.** 1988. Incubation periods in six models of intraperitoneally injected scrapie depend mainly on the dynamics of agent replication within the nervous system and not the lymphoreticular system. J. Gen. Virol. **69:**2953–2960.
26. **Kimberlin, R. H., and C. A. Walker.** 1989. The role of the spleen in the neuroinvasion of scrapie in mice. Virus Res. **12:**201–211.
27. **Llewelyn, C. A., P. E. Hewitt, R. S. Knight, K. Amar, S. Cousens, J. Mackenzie, and R. G. Will.** 2004. Possible transmission of variant Creutzfeldt-Jakob disease by blood transfusion. Lancet **363:**417–421.
28. **Mabbott, N. A., F. Mackay, F. Minns, and M. E. Bruce.** 2000. Temporary inactivation of follicular dendritic cells delays neuroinvasion of scrapie. Nat. Med. **6:**719–720.
29. **Mabbott, N. A., and G. G. MacPherson.** 2006. Prions and their lethal journey to the brain. Nat. Rev. Microbiol. **4:**201–211.
30. **Manson, J. C., E. Cancellotti, P. Hart, M. T. Bishop, and R. M. Barron.** 2006. The transmissible spongiform encephalopathies: emerging and declining epidemics. Biochem. Soc. Trans. **34:**1155–1158.
31. **Manson, J. C., A. R. Clarke, M. L. Hooper, L. Aitchison, I. McConnell, and J. Hope.** 1994. 129/Ola mice carrying a null mutation in PrP that abolishes mRNA production are developmentally normal. Mol. Neurobiol. **8:**121–127.
32. **Manson, J. C., A. R. Clarke, P. A. McBride, I. McConnell, and J. Hope.** 1994. PrP gene dosage determines the timing but not the final intensity or distribution of lesions in scrapie pathology. Neurodegeneration **3:**331–340.
33. **McBride, P. A., P. Eikelenboom, G. Kraal, H. Fraser, and M. E. Bruce.** 1992. PrP protein is associated with follicular dendritic cells of spleens and lymph nodes in uninfected and scrapie-infected mice. J. Pathol. **168:**413–418.
34. **McBride, P. A., W. J. Schulz-Schaeffer, M. Donaldson, M. Bruce, H. Diringer, H. A. Kretzschmar, and M. Beekes.** 2001. Early spread of scrapie from the gastrointestinal tract to the central nervous system involves autonomic fibers of the splanchnic and vagus nerves. J. Virol. **75:**9320–9327.
35. **Montrasio, F., R. Frigg, M. Glatzel, M. A. Klein, F. Mackay, A. Aguzzi, and C. Weissmann.** 2000. Impaired prion replication in spleens of mice lacking functional follicular dendritic cells. Science **288:**1257–1259.

36. **Peden, A. H., M. W. Head, D. L. Ritchie, J. E. Bell, and J. W. Ironside.** 2004. Preclinical vCJD after blood transfusion in a PRNP codon 129 heterozygous patient. Lancet **364:**527–529.
37. **Piccardo, P., J. C. Manson, D. King, B. Ghetti, and R. M. Barron.** 2007. Accumulation of prion protein in the brain that is not associated with transmissible disease. Proc. Natl. Acad. Sci. U. S. A. **104:**4712–4717.
38. **Prusiner, S. B.** 1998. Prions. Proc. Natl. Acad. Sci. U. S. A. **95:**13363–13383.
39. **Prusiner, S. B.** 1982. Novel proteinaceous infectious particles cause scrapie. Science **216:**136–144.
40. **Race, R., M. Oldstone, and B. Chesebro.** 2000. Entry versus blockade of brain infection following oral or intraperitoneal scrapie administration: role of prion protein expression in peripheral nerves and spleen. J. Virol. **74:**828–833.
41. **Rudd, P. M., M. R. Wormald, D. R. Wing, S. B. Prusiner, and R. A. Dwek.** 2001. Prion glycoprotein: structure, dynamics, and roles for the sugars. Biochemistry **40:**3759–3766.
42. **Sigurdson, C. J., C. Barillas-Mury, M. W. Miller, B. Oesch, L. J. van Keulen, J. P. Langeveld, and E. A. Hoover.** 2002. PrP(CWD) lymphoid cell targets in early and advanced chronic wasting disease of mule deer. J. Gen. Virol. **83:**2617–2628.
43. **Stimson, E., J. Hope, A. Chong, and A. L. Burlingame.** 1999. Site-specific characterization of the N-linked glycans of murine prion protein by high-performance liquid chromatography/electrospray mass spectrometry and exoglycosidase digestions. Biochemistry **38:**4885–4895.
44. **Taylor, P. R., M. C. Pickering, M. H. Kosco-Vilbois, M. J. Walport, M. Botto, S. Gordon, and L. Martinez-Pomares.** 2002. The follicular dendritic cell restricted epitope, FDC-M2, is complement C4; localization of immune complexes in mouse tissues. Eur. J. Immunol. **32:**1888–1896.
45. **Tuzi, N. L., E. Cancellotti, H. Baybutt, L. Blackford, B. Bradford, C. Plinston, A. Coghill, P. Hart, P. Piccardo, R. M. Barron, and J. C. Manson.** 2008. Host PrP glycosylation: a major factor determining the outcome of prion infection. PLoS Biol. **6:**e100.
46. **Will, R. G.** 2003. Acquired prion disease: iatrogenic CJD, variant CJD, kuru. Br. Med. Bull. **66:**255–265.
47. **Will, R. G., J. W. Ironside, M. Zeidler, S. N. Cousens, K. Estibeiro, A. Alperovitch, S. Poser, M. Pocchiari, A. Hofman, and P. G. Smith.** 1996. A new variant of Creutzfeldt-Jakob disease in the UK. Lancet **347:**921–925.
48. **Zanusso, G., D. Liu, S. Ferrari, I. Hegyi, X. Yin, A. Aguzzi, S. Hornemann, S. Liemann, R. Glockshuber, J. C. Manson, P. Brown, R. B. Petersen, P. Gambetti, and M. S. Sy.** 1998. Prion protein expression in different species: analysis with a panel of new mAbs. Proc. Natl. Acad. Sci. U. S. A. **95:**8812–8816.